Supplementary Material for

Absolute Pose Estimation from Line Correspondences using Direct Linear Transformation

Bronislav Přibyl Pavel Zemčík Martin Čadík

Brno University of Technology, Faculty of Information Technology, Centre of Excellence IT4Innovations
Božetěchova 2, 612 66 Brno, Czech Republic

February 7, 2017

This supplementary material contains boxplots visualizing distributions of errors of individual PnL methods. Each distribution over 1000 trials is depicted by a box, where

- black dot inside a mark = median,
- box body = interquartile range (IQR),
- whiskers = minima and maxima in the interval of 10× IQR, and
- isolated dots = outliers.

1 Robustness to image noise

Figures 1 – 15 depict errors in estimated camera pose as a function of the number of lines (from 3 to 10,000). The following methods were tested. Each method is assigned a different color and shape in the figures.

- ▶ **Ansar**, the method by Ansar and Daniilidis (2003), implementation from Xu et al. (2016).
- ● **Mirzaei**, the method by Mirzaei and Roumeliotis (2011).
- ◆ **RPnL**, the method by Zhang et al. (2013).
- ◆ **ASPnL**, the method by Xu et al. (2016).
- ★ **LPnL_Bar_LS**, the method by Xu et al. (2016).
- ✶ **LPnL_Bar_ENull**, the method by Xu et al. (2016).
- ▲ **DLT-Lines**, the method by Hartley and Zisserman (2004, p. 180), our implementation.
- ▼ **DLT-Plücker-Lines**, the method by Přibyl et al. (2015), our implementation.
- ■ **DLT-Combined-Lines**, the proposed method.

Figures 1 – 5 depict errors in estimated camera orientation $\Delta\Theta$ [°] for increasing levels of image noise with standard deviation $\sigma = 1, 2, 5, 10$ and 20 pixels. Accordingly, Figures 6 – 10 depict errors in estimated camera position ΔT [m], and Figures 11 – 15 depict reprojection errors $\Delta\pi$ [ ].

2 Robustness to quasi-singular cases

The methods were evaluated in three quasi-singular scenarios:

- Limited number of line directions (2 random directions, 3 random directions, 3 orthogonal directions) – Figure 16.
- Near-planar lines – Figure 17.
- Near-concurrent lines – Figure 18.

3 Robustness to outliers

Figure 19 depicts errors in estimated camera pose as a function of the fraction of outliers, out of total 500 line correspondences. Legend is provided in the figure itself.

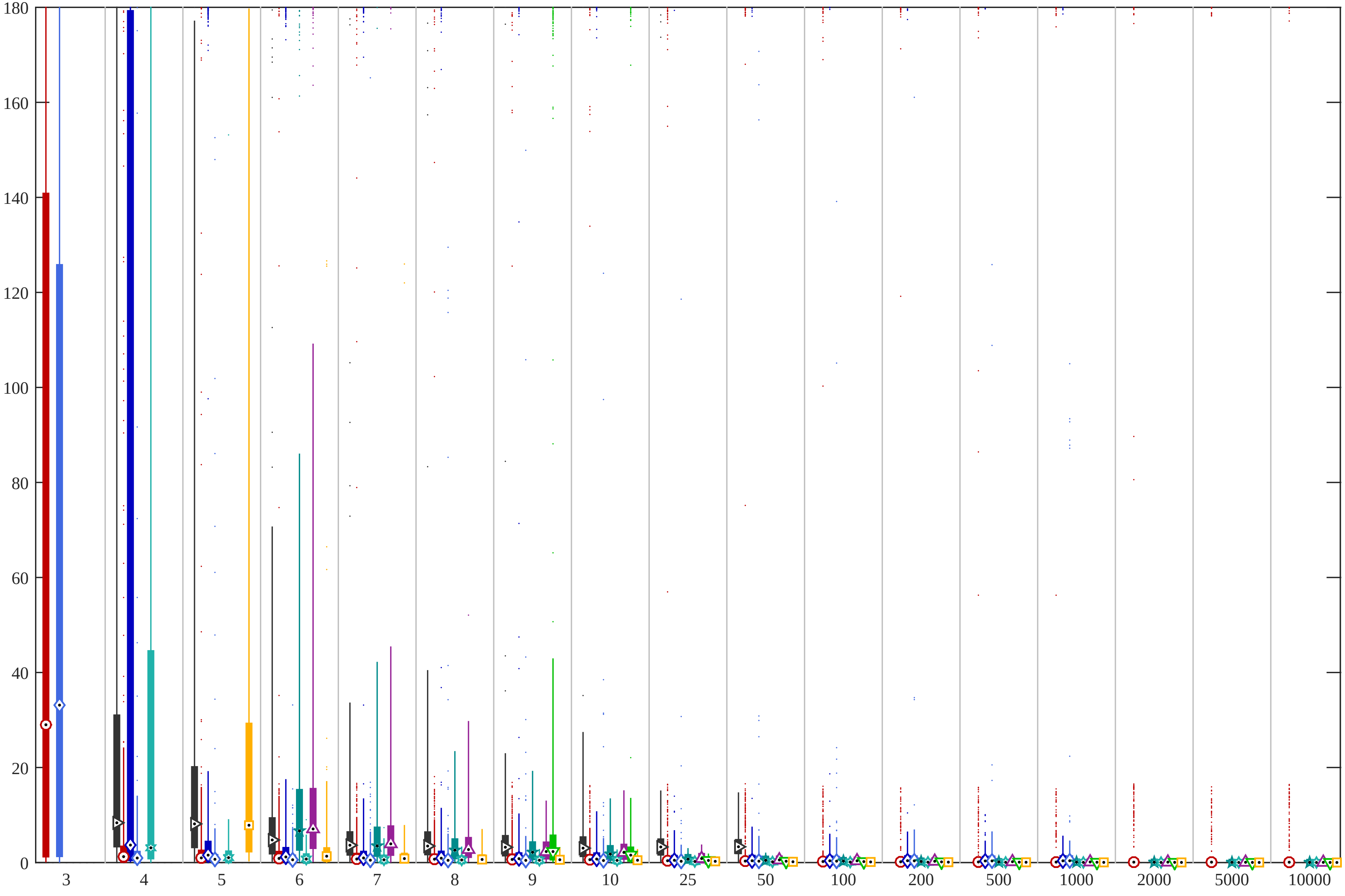

Figure 1: Errors in camera orientation $\Delta\Theta$ [°] for image noise with standard deviation $\sigma = 1$ pixel.

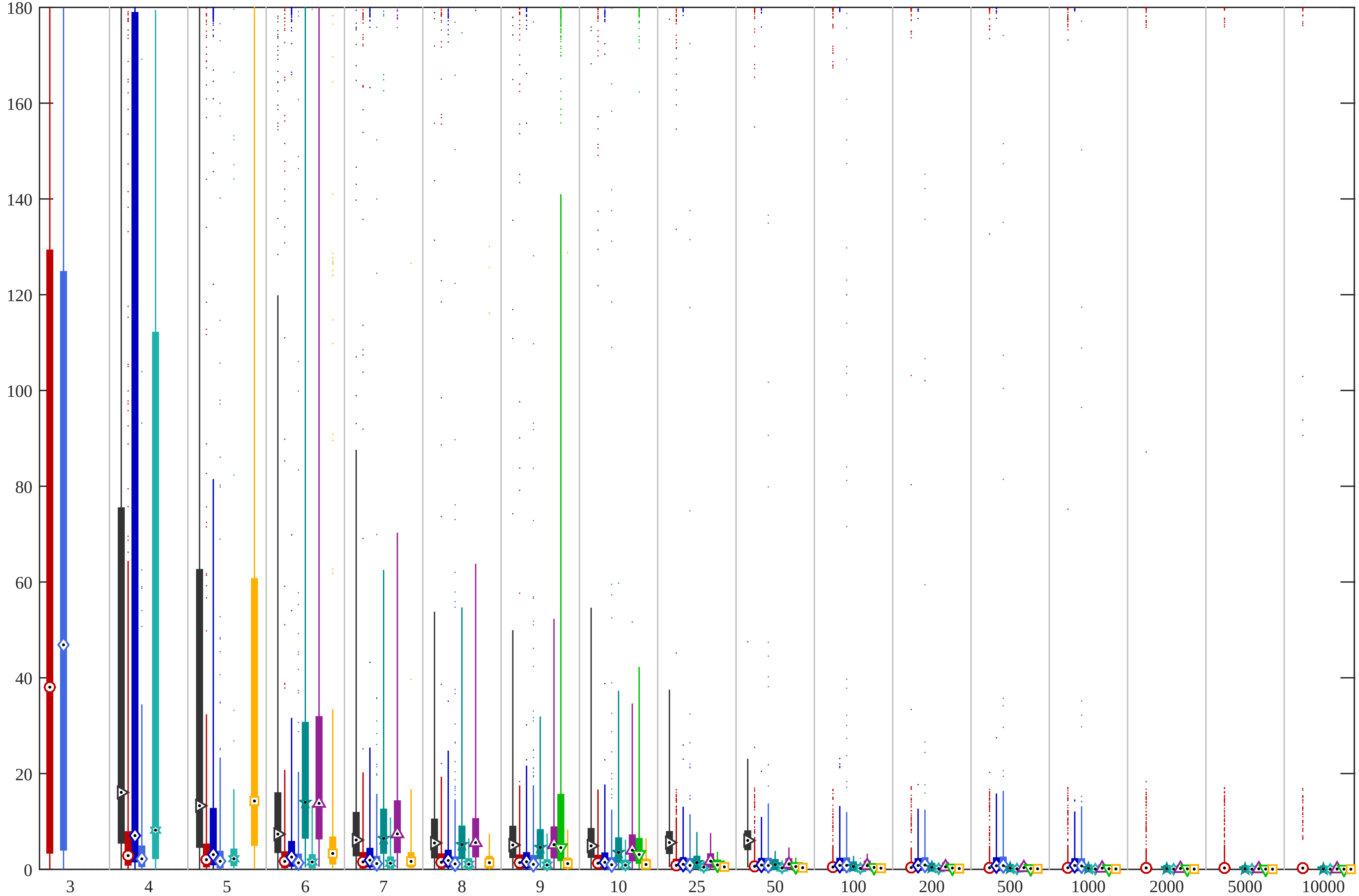

Figure 2: Errors in camera orientation $\Delta\Theta$ [°] for image noise with standard deviation $\sigma = 2$ pixels.

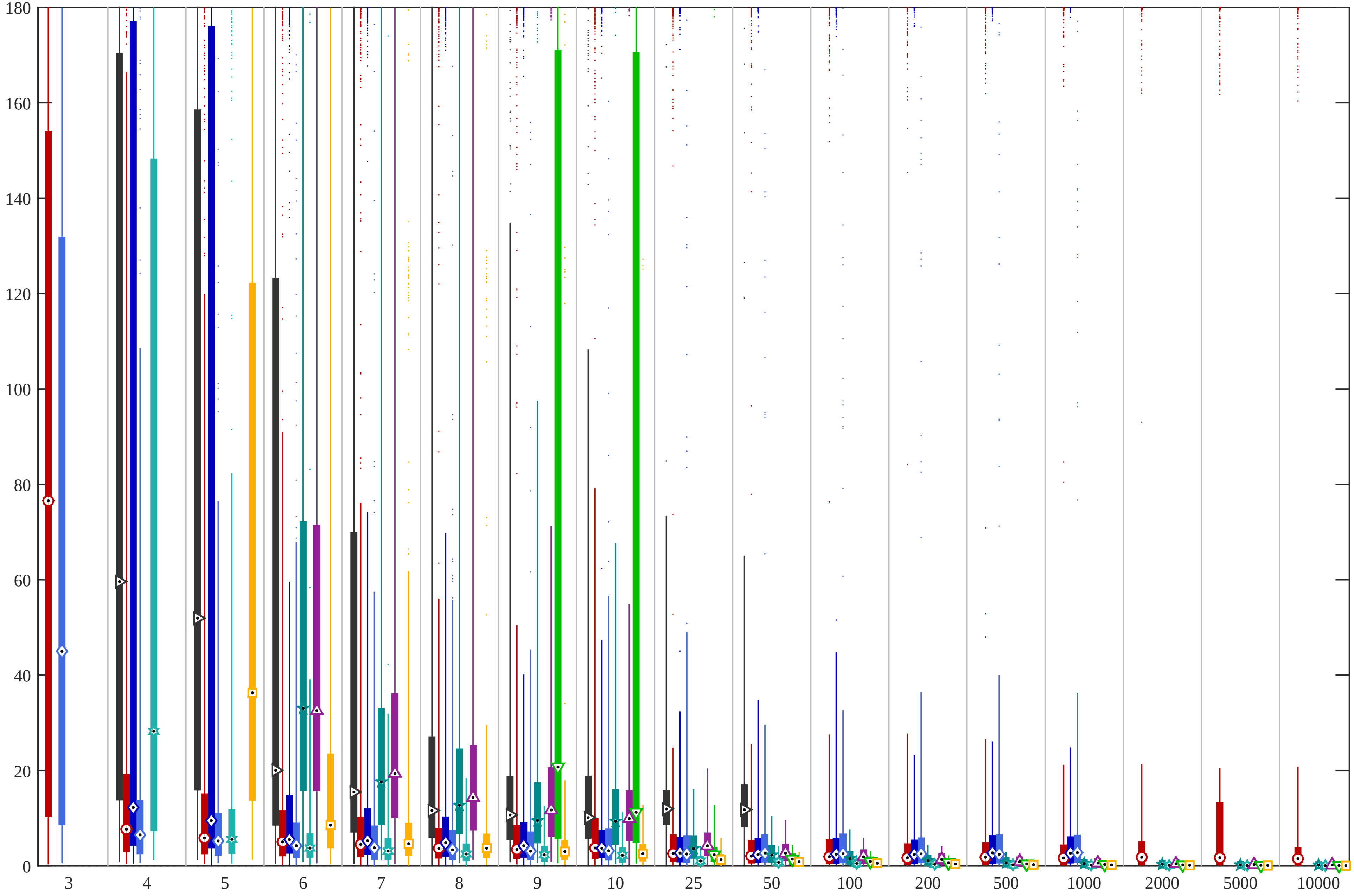

Figure 3: Errors in camera orientation $\Delta\Theta$ [°] for image noise with standard deviation $\sigma = 5$ pixels.

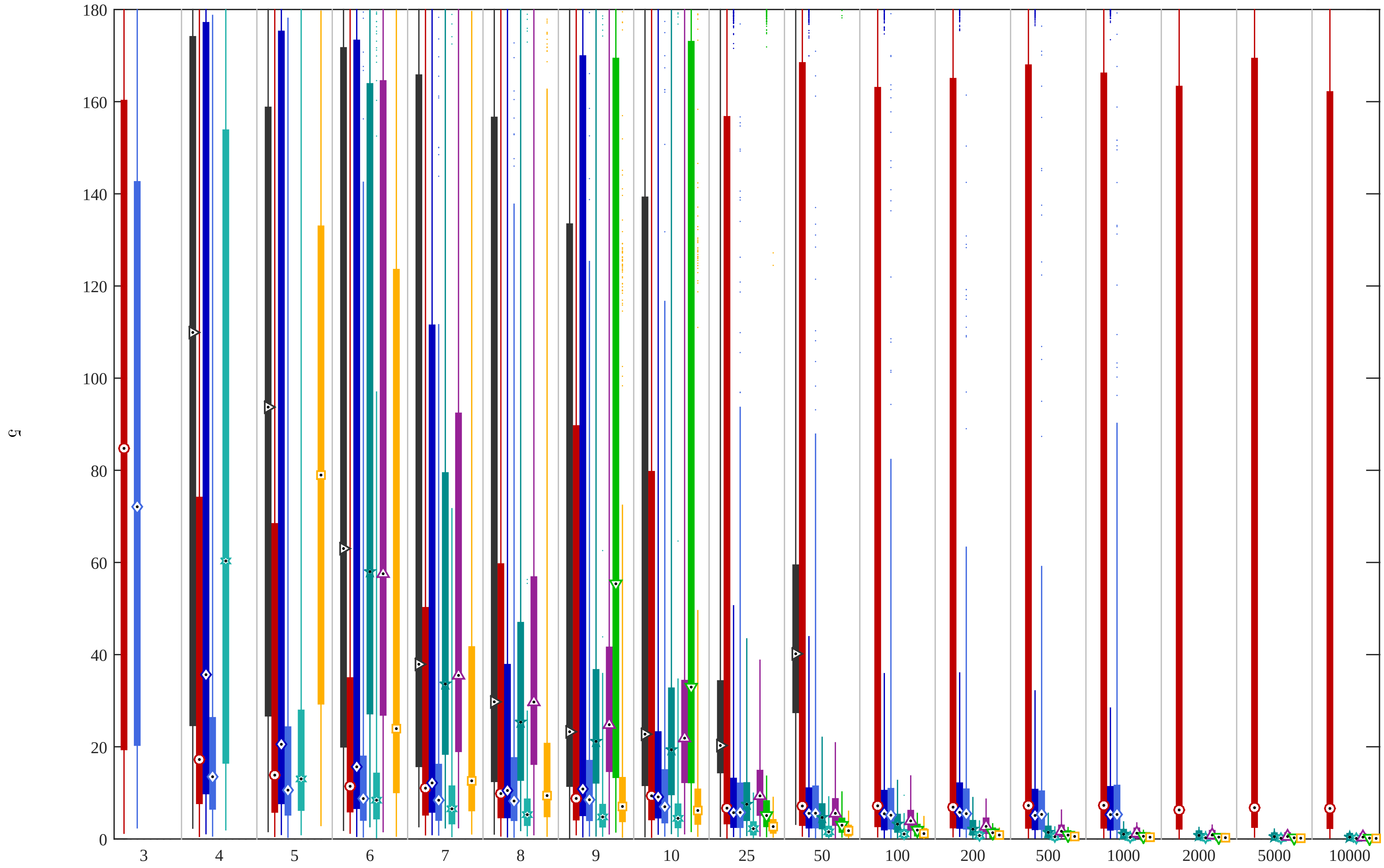

Figure 4: Errors in camera orientation $\Delta\Theta$ [°] for image noise with standard deviation $\sigma = 10$ pixels.

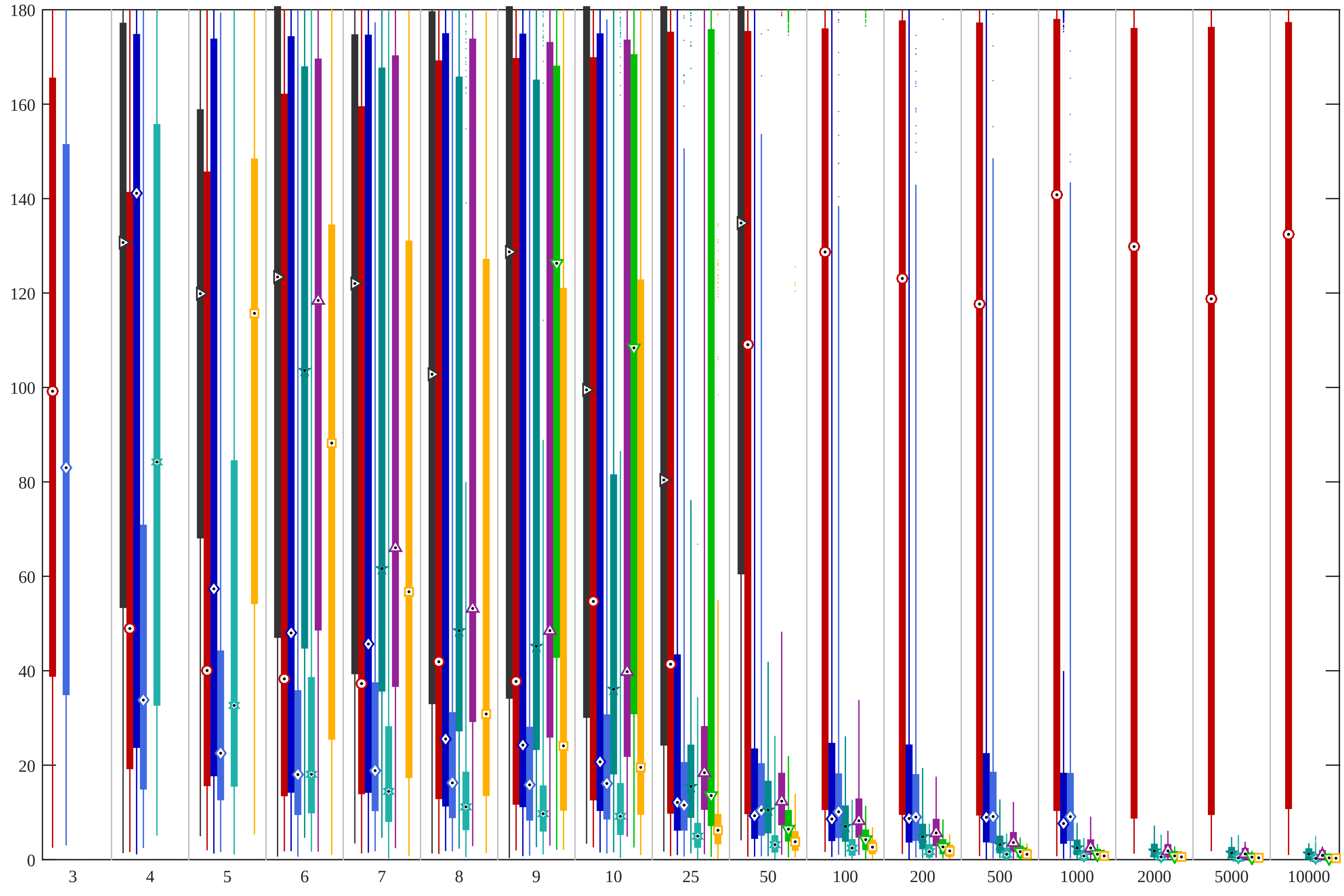

Figure 5: Errors in camera orientation $\Delta\Theta$ [°] for image noise with standard deviation $\sigma = 20$ pixels.

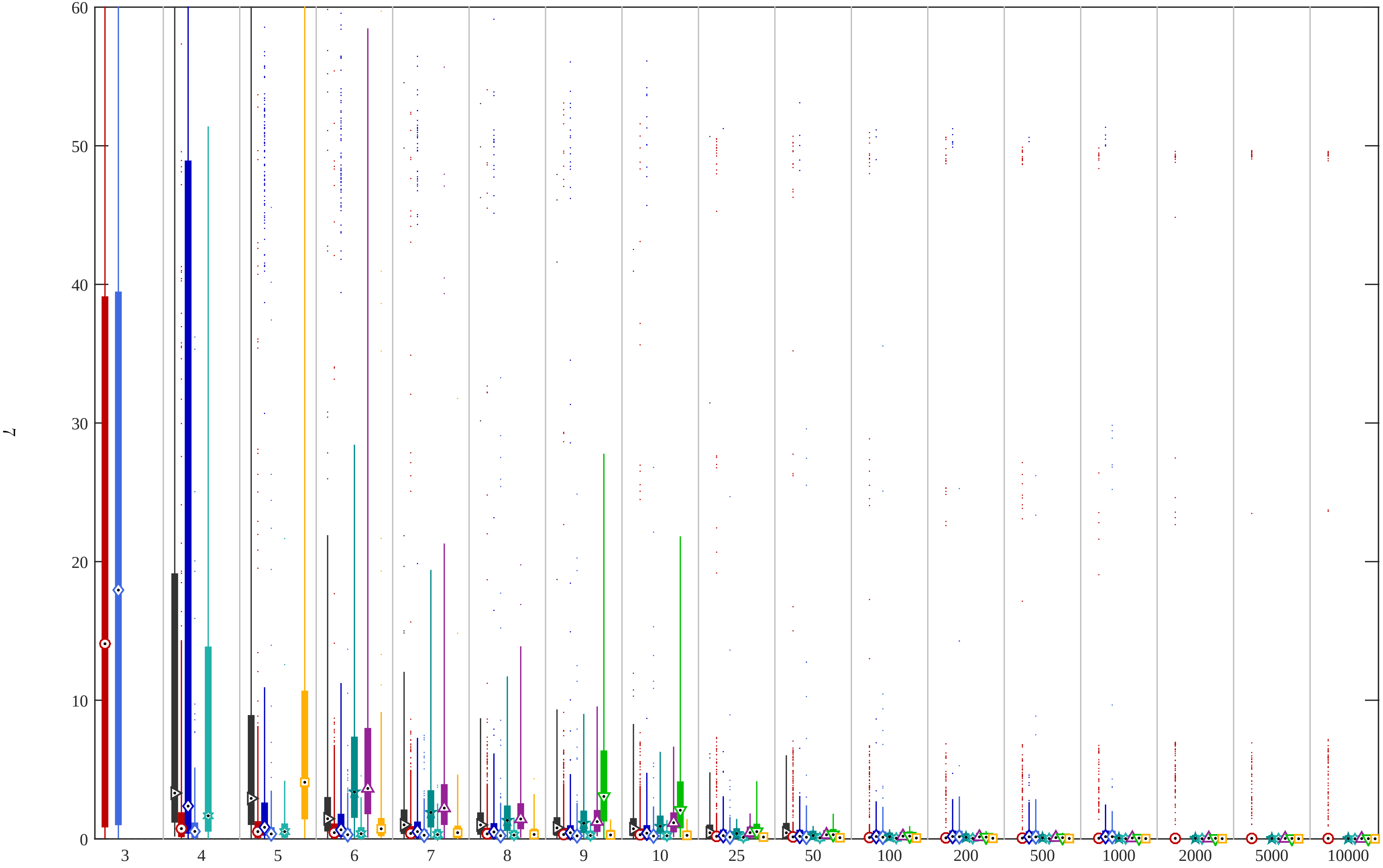

Figure 6: Errors in camera position ΔT [m] for image noise with standard deviation $\sigma = 1$ pixel.

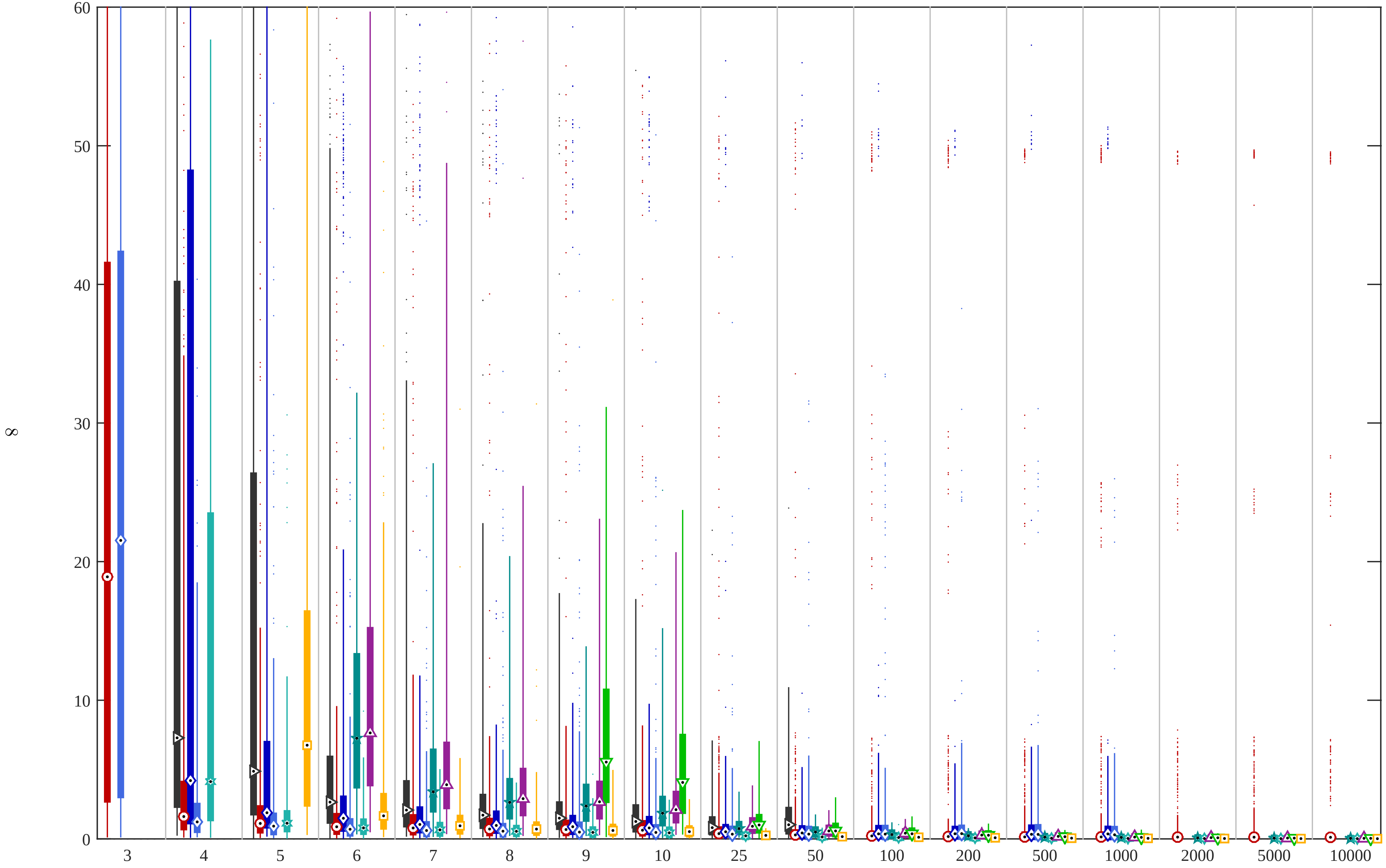

Figure 7: Errors in camera position ΔT [m] for image noise with standard deviation $\sigma = 2$ pixels.

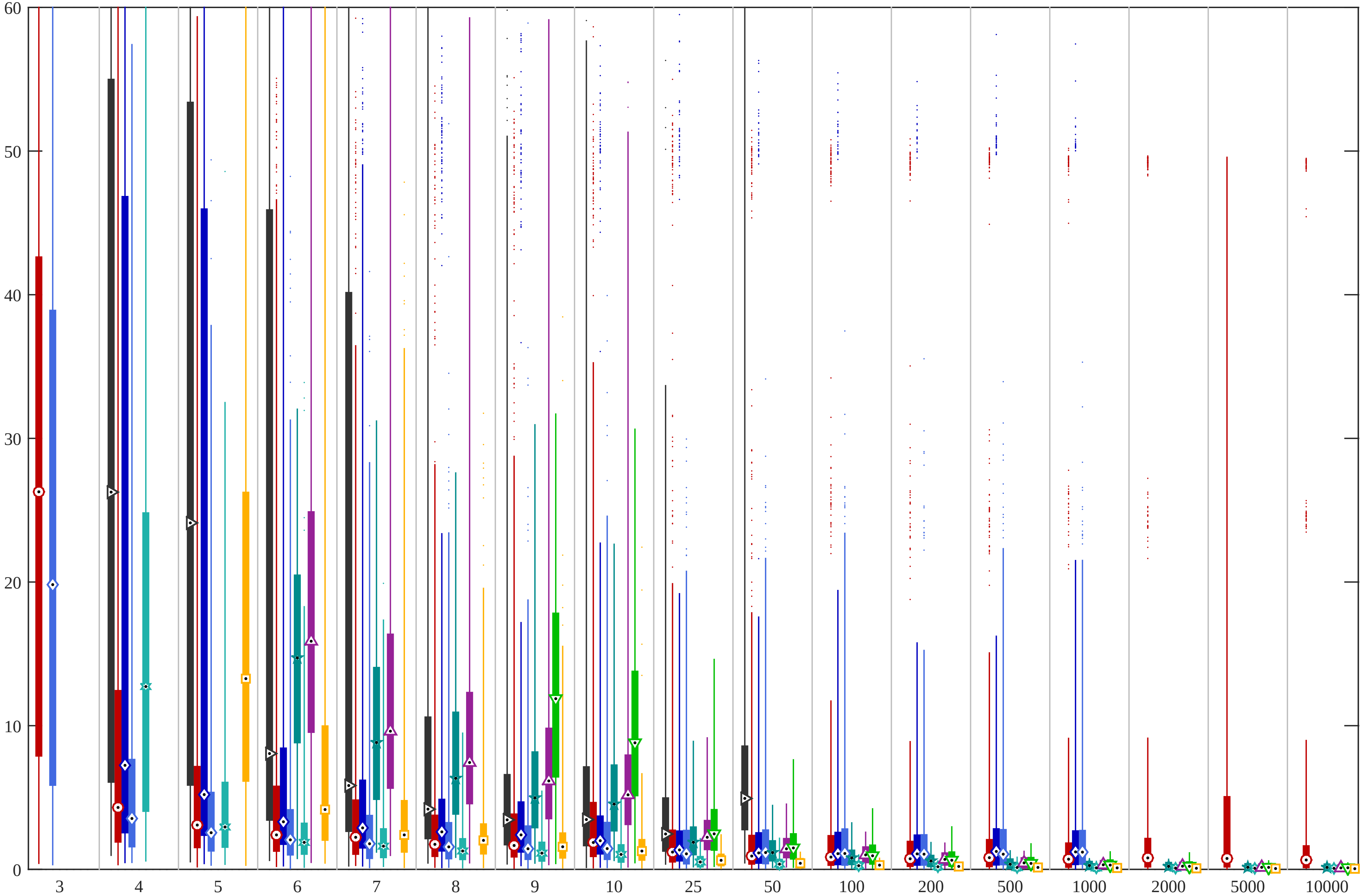

Figure 8: Errors in camera position ΔT [m] for image noise with standard deviation $\sigma = 5$ pixels.

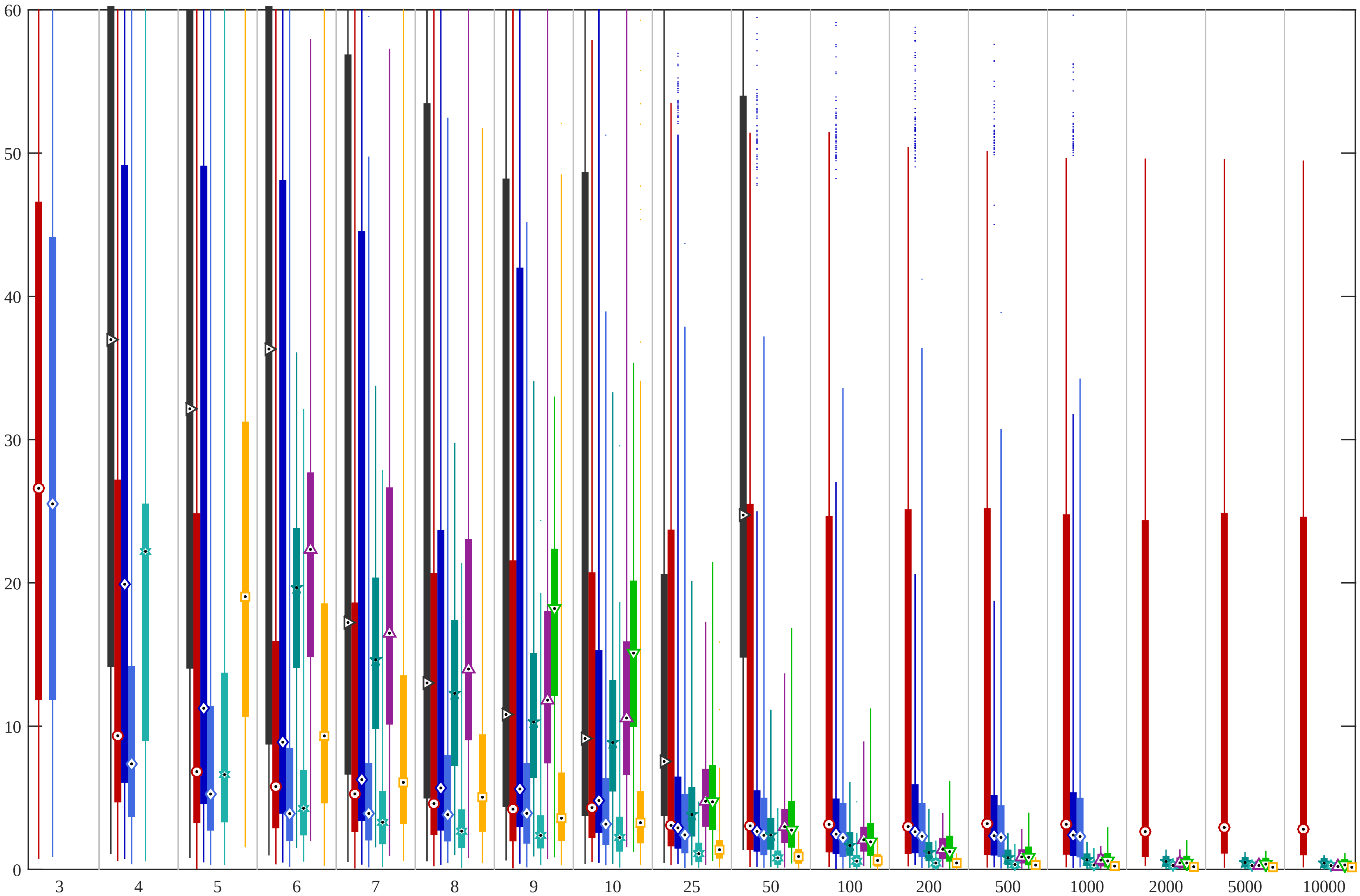

Figure 9: Errors in camera position ΔT [m] for image noise with standard deviation $\sigma = 10$ pixels.

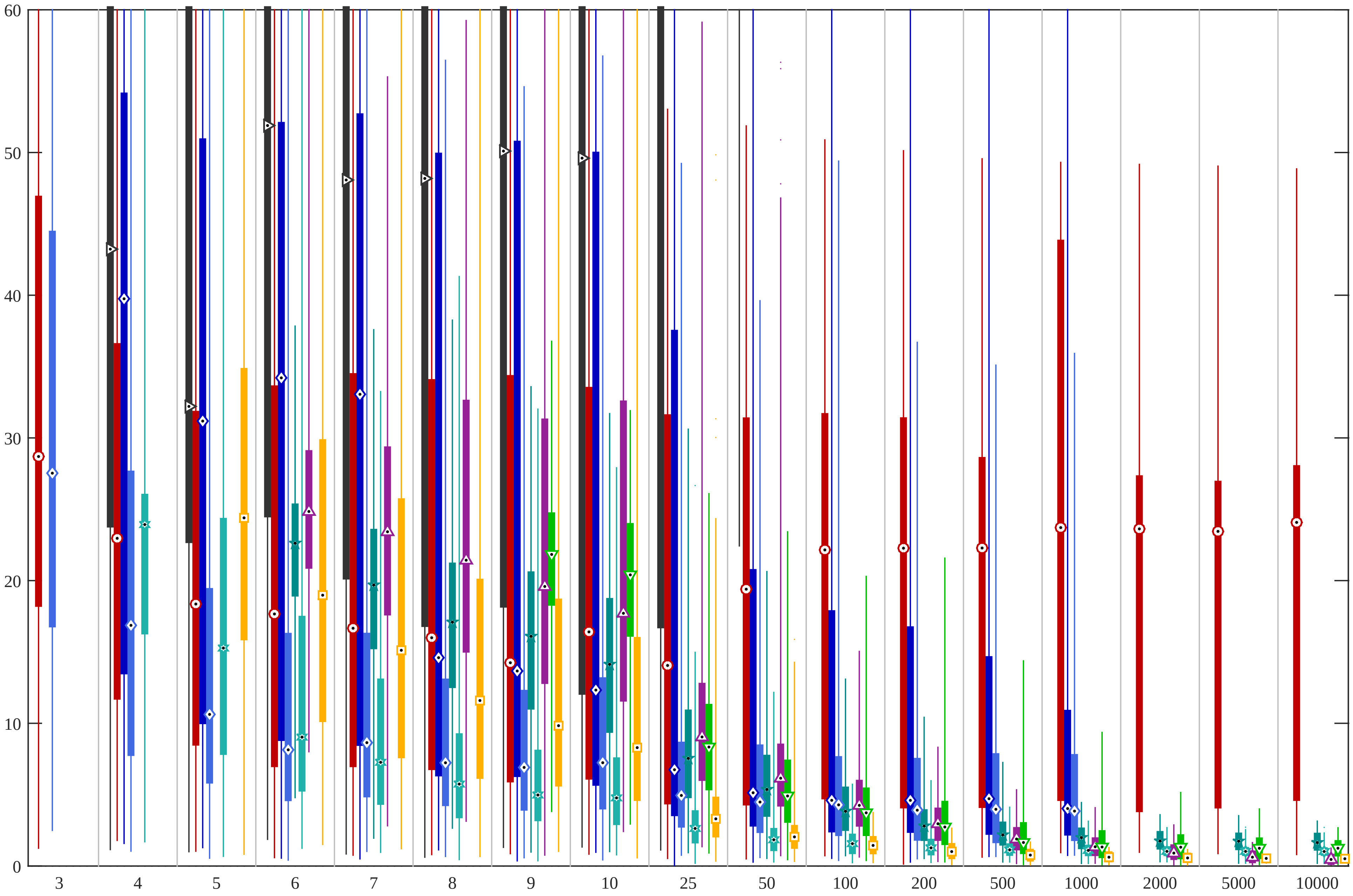

Figure 10: Errors in camera position ΔT [m] for image noise with standard deviation $\sigma = 20$ pixels.

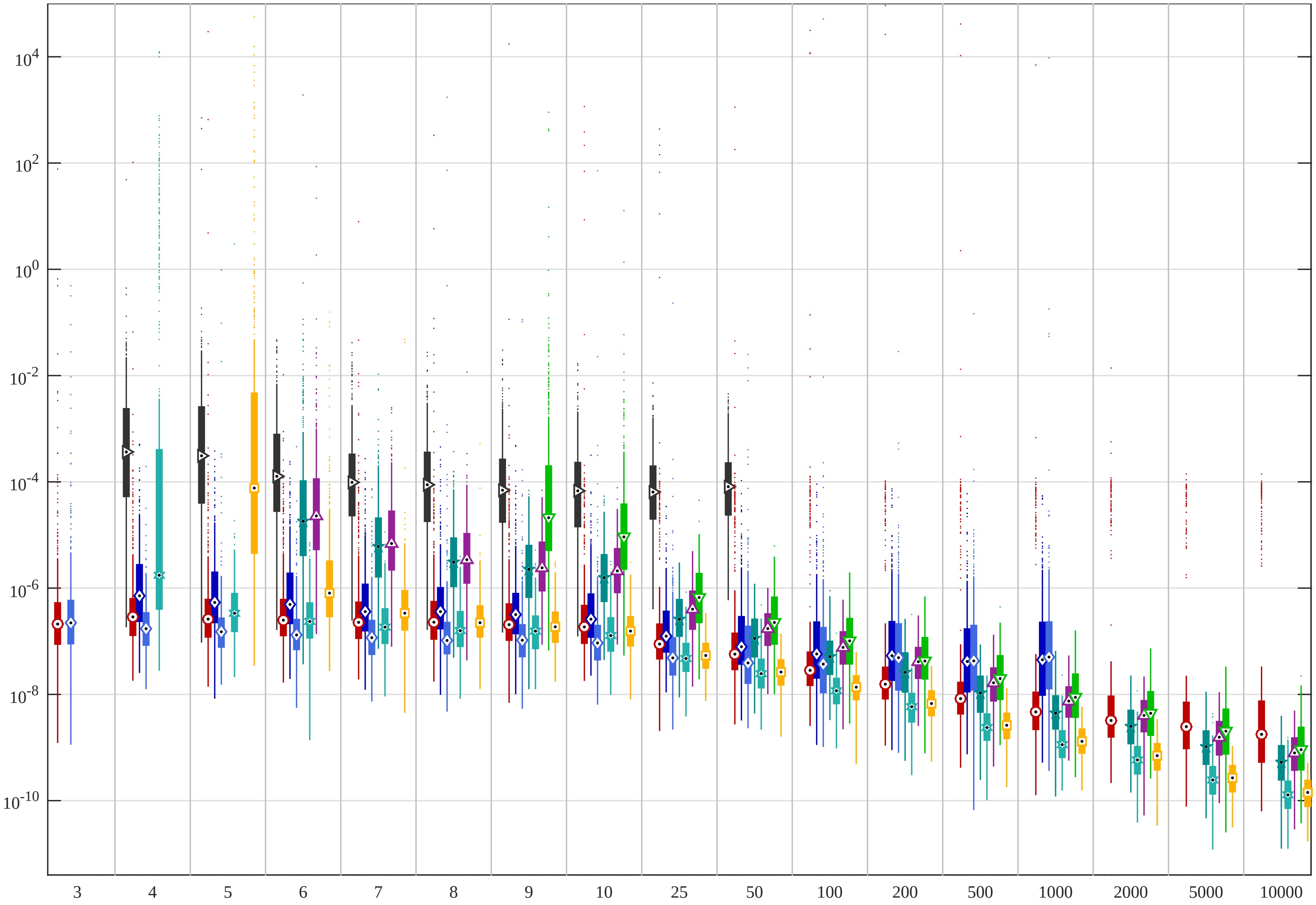

Figure 11: Reprojection errors $\Delta\pi$ [] for image noise with standard deviation $\sigma = 1$ pixel.

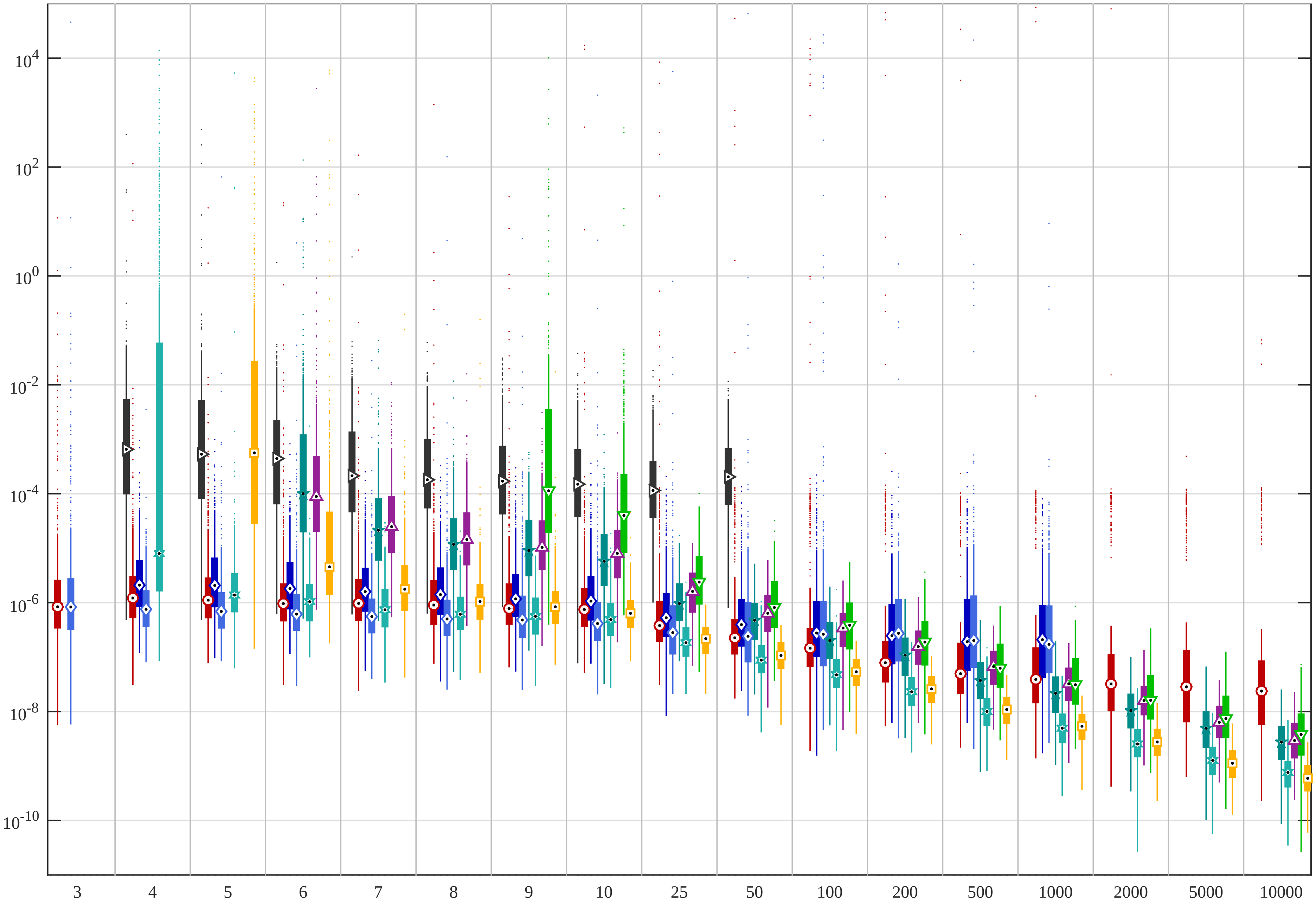

Figure 12: Reprojection errors $\Delta\pi$ [] for image noise with standard deviation $\sigma = 2$ pixels.

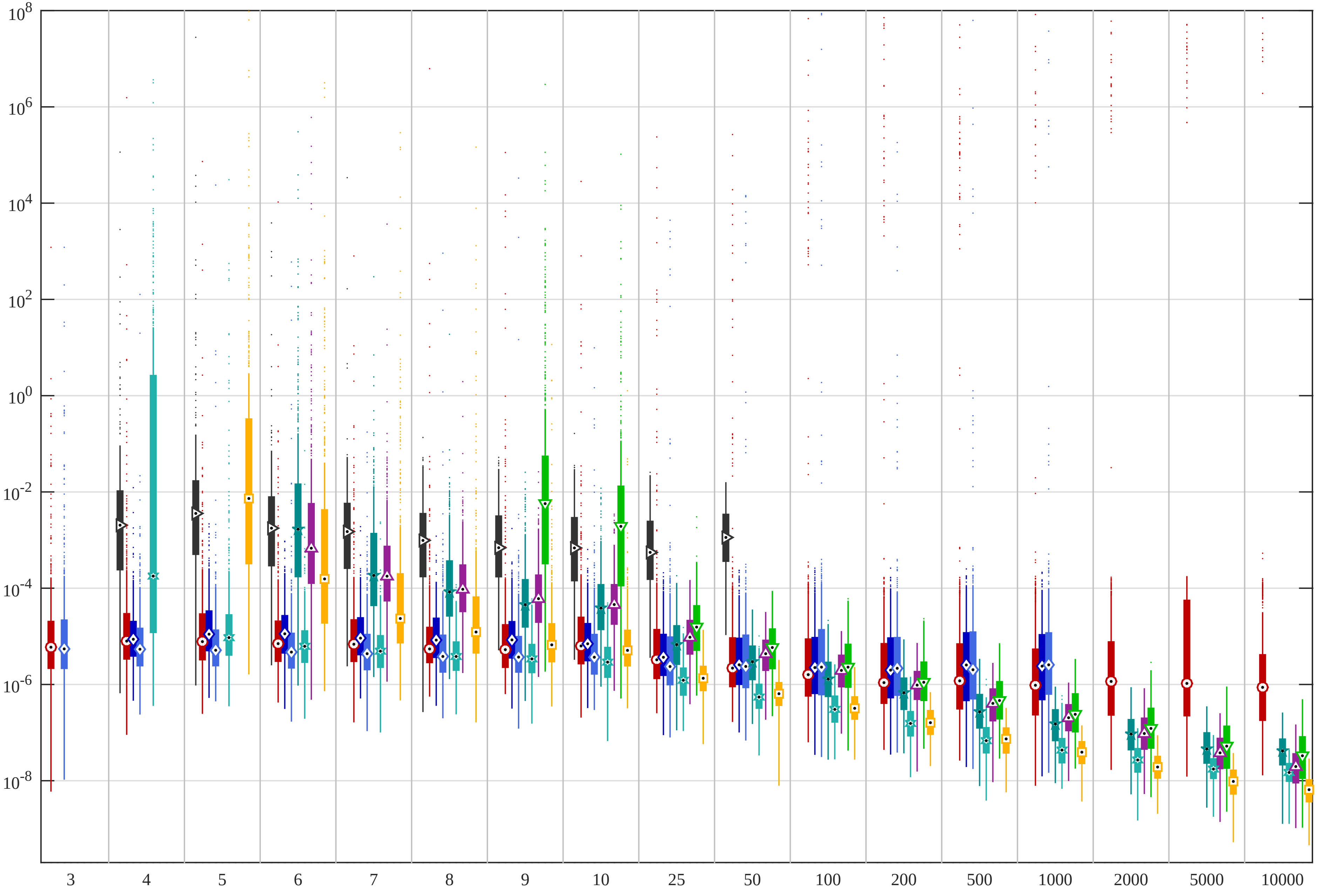

Figure 13: Reprojection errors $\Delta\pi$ [] for image noise with standard deviation $\sigma = 5$ pixels.

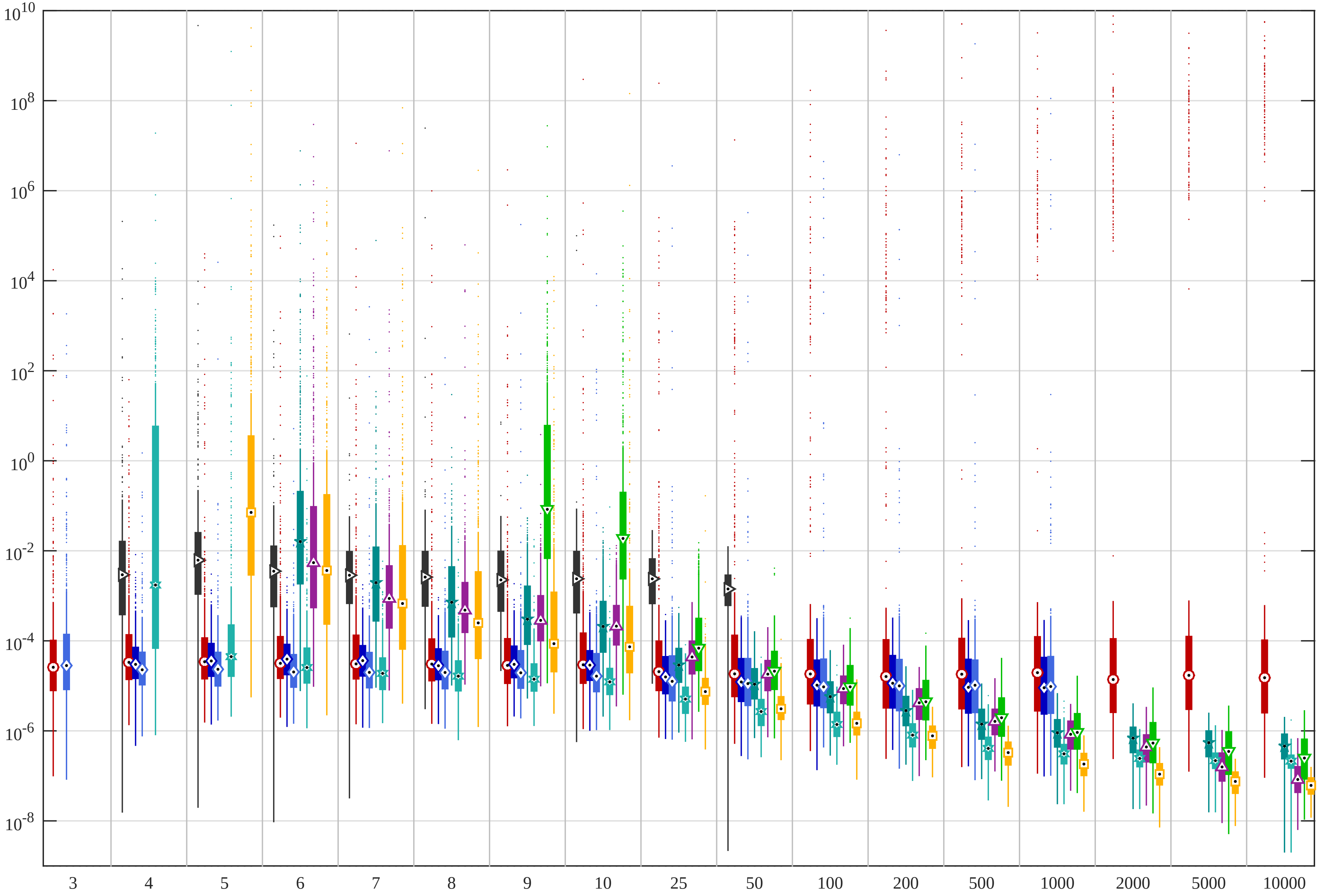

Figure 14: Reprojection errors $\Delta\pi$ [] for image noise with standard deviation $\sigma = 10$ pixels.

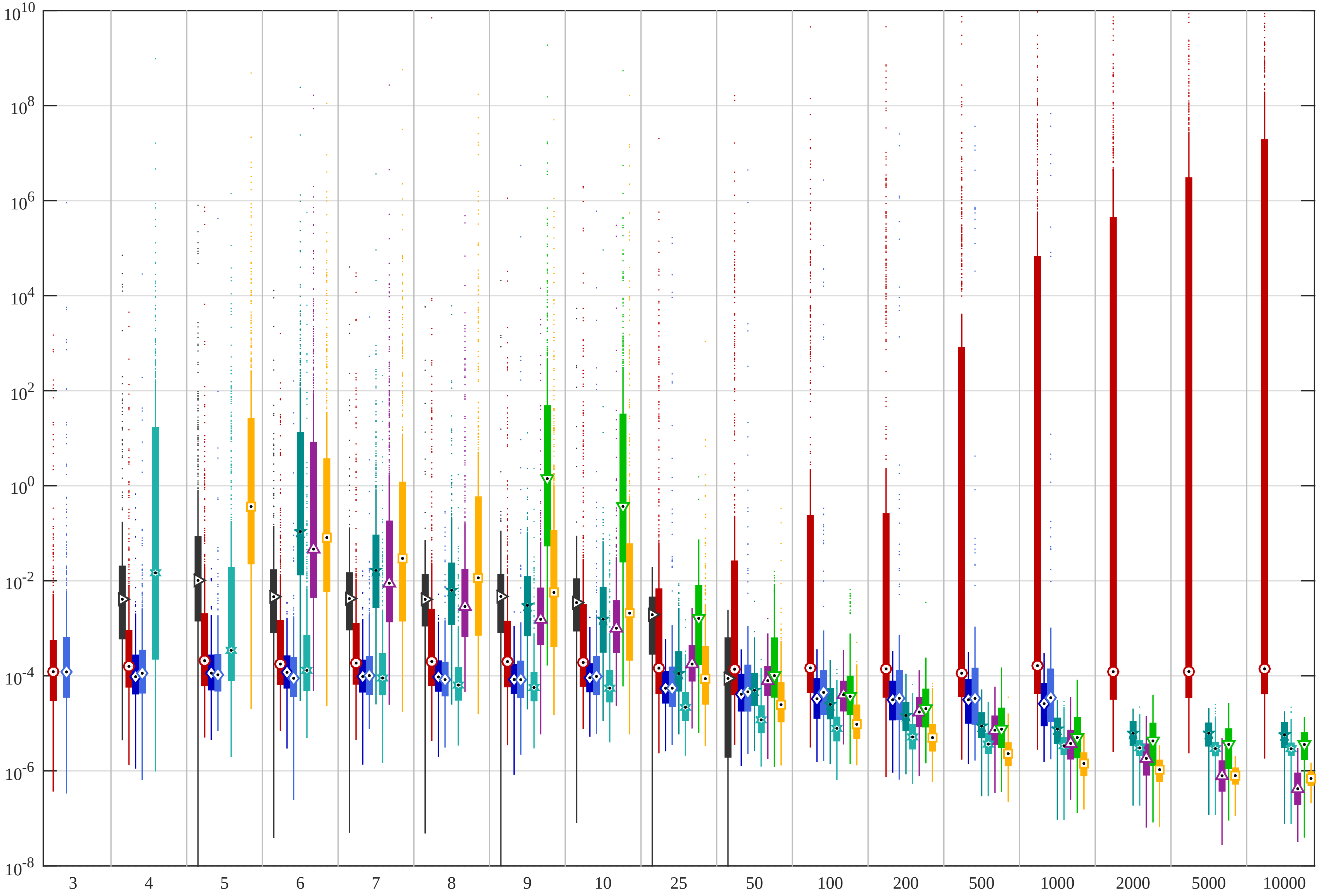

Figure 15: Reprojection errors $\Delta\pi$ [] for image noise with standard deviation $\sigma = 20\,$pixels.

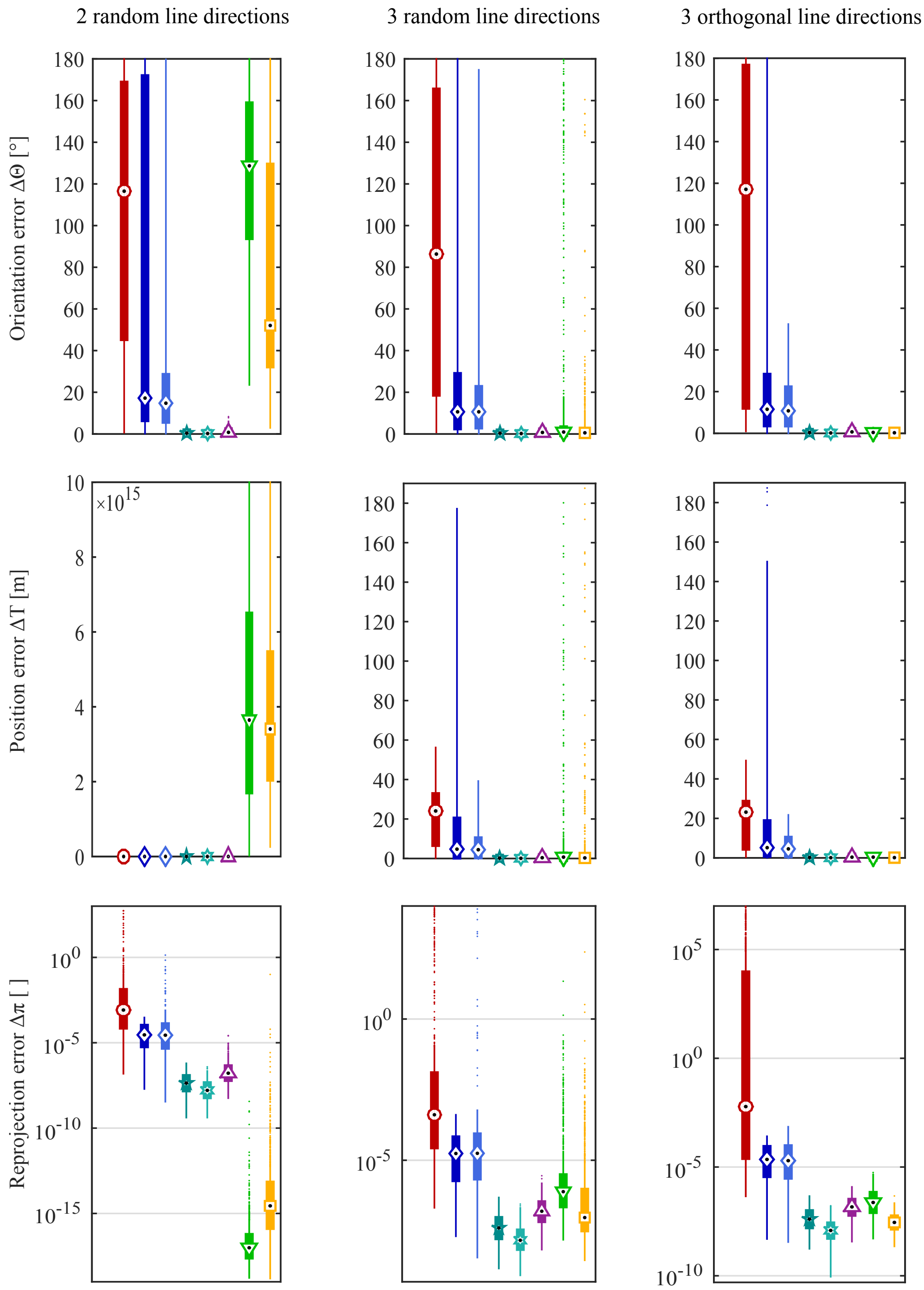

Figure 16: Robustness to quasi-singular cases. The distribution of orientation errors ($\Delta\Theta$, *top*), position errors ($\Delta\mathrm{T}$, *middle*) and reprojection errors ($\Delta\pi$, *bottom*) for the case with 2 random line directions (*left*), 3 random line directions (*center*) and 3 orthogonal line directions (*right*). Number of lines was $m = 200$ and standard deviation of image noise was $\sigma = 2$ pixels.

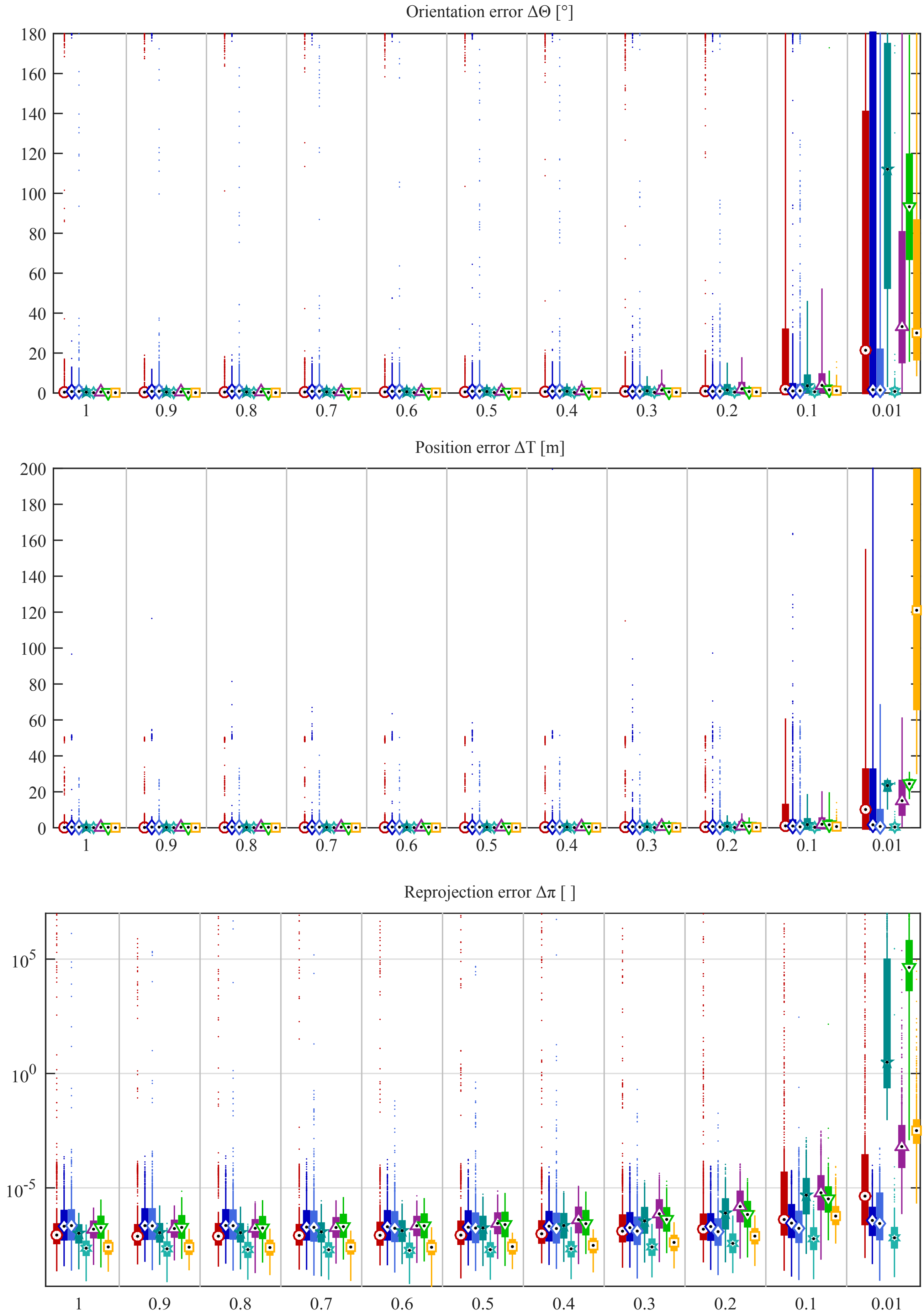

Figure 17: Robustness to near-planar line distribution. The distribution of orientation errors ($\Delta\Theta$, *top*), position errors ($\Delta\mathrm{T}$, *middle*) and reprojection errors ($\Delta\pi$, *bottom*) as a function of 'flatness' (the ratio of height of a volume containing 3D lines w. r. t. to its remaining dimensions). Number of lines was $m = 200$ and standard deviation of image noise was $\sigma = 2$ pixels.

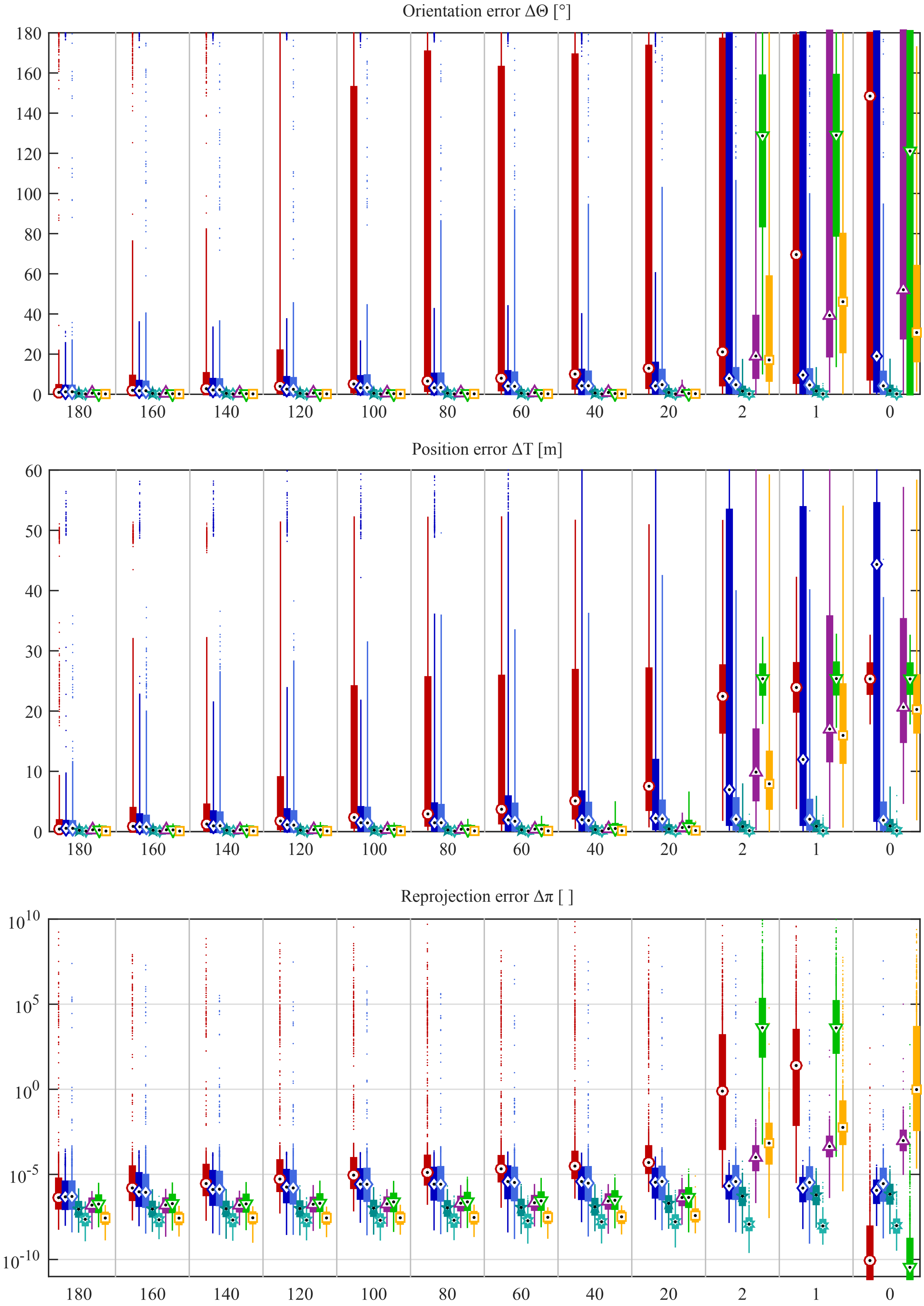

Figure 18: Robustness to near-concurrent line distribution. The distribution of orientation errors ($\Delta\Theta$, *top*), position errors ($\Delta\mathrm{T}$, *middle*) and reprojection errors ($\Delta\pi$, *bottom*) as a function of the number of lines, which are not concurrent, out of all $m = 200$ lines. Standard deviation of image noise was $\sigma = 2$ pixels.

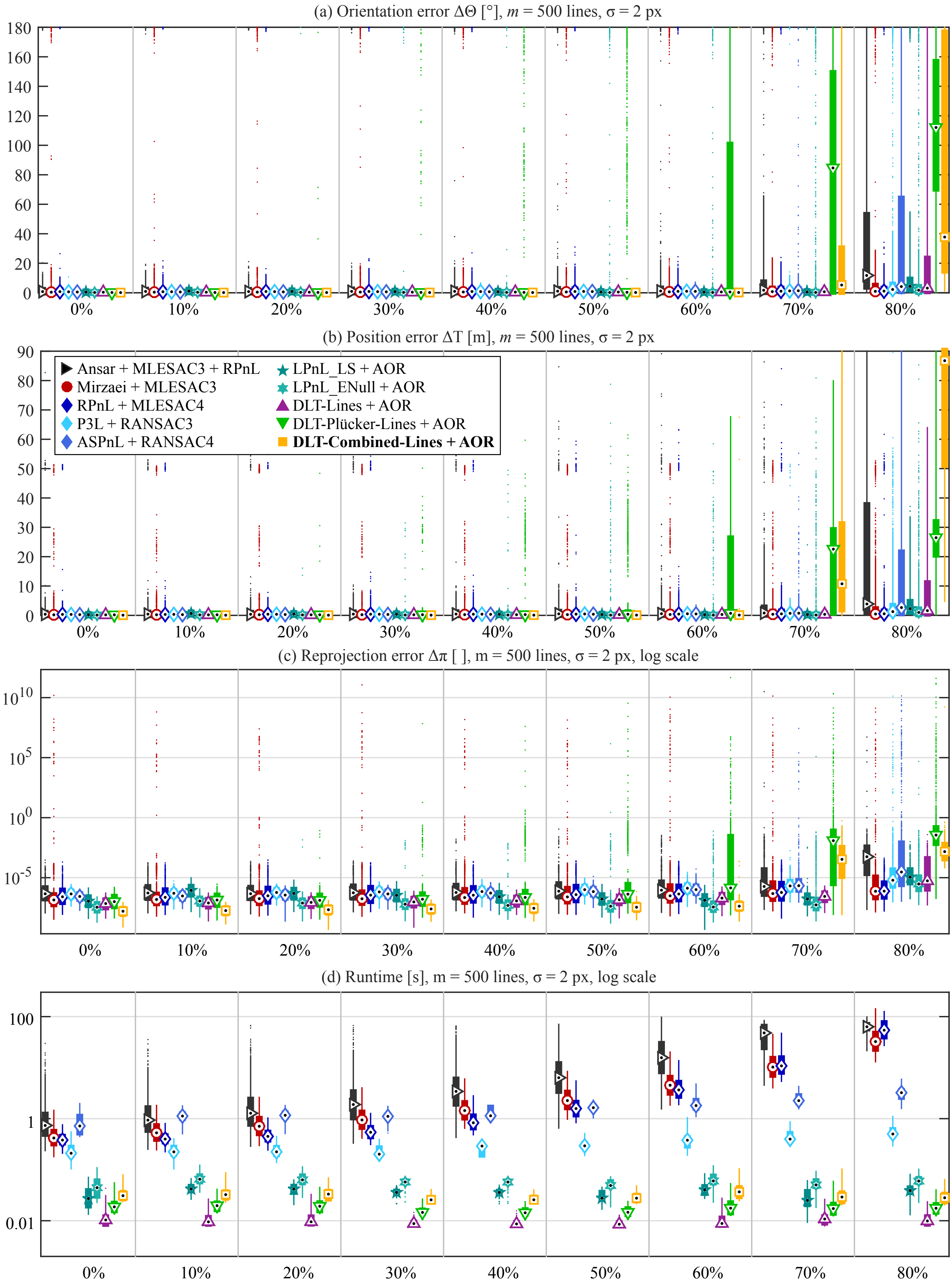

Figure 19: Robustness to outliers. The distribution of orientation errors ($\Delta\Theta$, a), position errors ($\Delta\mathrm{T}$, b), reprojection errors ($\Delta\pi$, c) and runtimes (d) as a function of the fraction of outliers, out of total 500 line correspondences.

References

Ansar A, Daniilidis K. Linear pose estimation from points or lines. IEEE Transactions on Pattern Analysis and Machine Intelligence 2003;25(5):578–89. doi:10.1109/TPAMI.2003.1195992.

Hartley RI, Zisserman A. Multiple View Geometry in Computer Vision. 2nd ed. Cambridge University Press, 2004. doi:10.1017/CBO9780511811685.

Mirzaei FM, Roumeliotis SI. Globally optimal pose estimation from line correspondences. In: IEEE International Conference on Robotics and Automation 2011. IEEE; 2011. p. 5581–8. doi:10.1109/ICRA.2011.5980272.

Přibyl B, Zemčík P, Čadík M. Camera pose estimation from lines using plücker coordinates. In: Proceedings of the British Machine Vision Conference (BMVC 2015). The British Machine Vision Association and Society for Pattern Recognition; 2015. p. 1–12. doi:10.5244/C.29.45.

Xu C, Zhang L, Cheng L, Koch R. Pose estimation from line correspondences: A complete analysis and a series of solutions. IEEE Transactions on Pattern Analysis and Machine Intelligence 2016;doi:10.1109/TPAMI.2016.2582162.

Zhang L, Xu C, Lee KM, Koch R. Robust and efficient pose estimation from line correspondences. In: Asian Conference on Computer Vision 2012. Springer; 2013. p. 217–30. doi:10.1007/978-3-642-37431-9_17.

Acknowledgements

This work was supported by The Ministry of Education, Youth and Sports of the Czech Republic from the National Programme of Sustainability (NPU II); project IT4Innovations excellence in science – LQ1602.